Metrologia **46** (2009) 409–415 doi:10.1088/0026-1394/46/5/004

A Johnson noise thermometer with traceability to electrical standards

Luca Callegaro, Vincenzo D'Elia, Marco Pisani and Alessio Pollarolo

INRIM—Istituto Nazionale di Ricerca Metrologica, Strada delle Cacce, 91, 10135 Torino, Italy

Received 30 January 2009, in final form 29 April 2009
Published 24 June 2009
Online at stacks.iop.org/Met/46/409

Abstract
The paper presents an absolute Johnson noise thermometer (JNT), an instrument to measure the thermodynamic temperature of a sensing resistor, with traceability to voltage, resistance and frequency quantities. The temperature is measured in energy units, and can be converted to SI units (kelvin) with the accepted value of the Boltzmann constant k_B; or, conversely, it can be employed to perform measurements at the triple point of water and obtain a determination of k_B. The thermometer is composed of a correlation spectrum analyzer and a calibrator. The calibrator generates a pseudorandom noise (at a level suitable for traceability to an ac voltage standard) by digital synthesis, scaled in amplitude by a chain of electromagnetic voltage dividers and cyclically injected in series with the Johnson noise. First JNT measurements at room temperature are compatible with those of a standard platinum resistance thermometer within the estimated combined uncertainty of $60\,\mu\mathrm{K\,K^{-1}}$ of both instruments. A path towards future improvements of JNT accuracy is also sketched.

1. Introduction

The accurate measurement of Johnson noise has been considered a method for determining the thermodynamic temperature, and the Boltzmann constant k_B, since its very first observation [1]. A resistor R, in thermodynamic equilibrium, generates a noise voltage $v(t)$ with the spectral power density[1] $S_v^2 = 4R\mathcal{T}$, where $\mathcal{T}$ is its thermodynamic temperature measured in energy units.

Within the International System of units, with the quantity temperature T a base unit is associated, the kelvin (K), defined by assigning the temperature of the triple point of water (TPW), $T_{TPW} = 273.16$ K; the relation $\mathcal{T}_{TPW} = k_B T_{TPW}$ defines k_B. In an effort towards a possible redefinition of the kelvin, in 2005 the Consultative Committee for Thermometry (CCT) of the International Committee for Weights and Measures (CIPM) [2] recommended to 'initiate and continue experiments to determine values of thermodynamic temperature and the Boltzmann constant'.

Johnson noise thermometry experiments have the potential for such new determinations. A detailed analysis suggests [3] the possibility of achieving a k_B relative uncertainty of a few parts in 10^6, comparable to the estimated or forecasted uncertainties of other existing or proposed experiments [4].

In the following, we present a Johnson noise thermometer (JNT) which measures $\mathcal{T}$ with traceability to national standards of ac voltage, resistance and frequency. The thermometer is composed of a correlation spectrum analyzer and a calibrator. The calibrator generates by digital synthesis a pseudorandom noise (at a level suitable for traceability to an ac voltage standard), scaled in amplitude by a chain of electromagnetic voltage dividers and cyclically injected in series with the Johnson noise (thus avoiding the standard solution of a mechanical switch at the spectrum analyzer input).

If k_B is taken as given (in the following the CODATA 2006 adjustment [5, 6] will be employed) the JNT measurement outcome can be compared with an ITS-90 temperature T_{90} measurement taken as reference.

Presently, the JNT has been tested by performing measurements near room temperature. A measurement run at room temperature gives T in agreement with T_{90} within the combined relative measurement uncertainty around $60\,\mu\mathrm{K\ K^{-1}}$. Several uncertainty contributions are related to the use of commercial instrumentation. In the future, purposely built instruments under development will permit a

[1] The expression is accurate to one part in 10^7 at room temperature and frequency below 1 MHz.

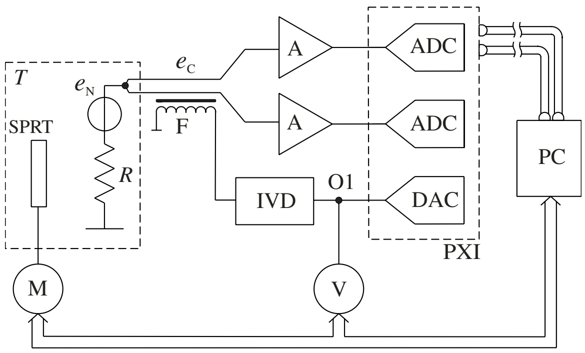

Figure 1. Block schematics of the JNT; see text for details.

significant accuracy improvement, and will open the possibility of employing the JNT for a new determination of k_B.

2. Absolute and relative measurements

The main difficulty in the development of an accurate JNT is the faintness of the Johnson noise, which must be amplified by a large factor (10^4 to 10^6). Noise added by front-end amplifiers has an amplitude comparable with that of the Johnson noise itself, but can be rejected with the correlation technique (see [7, paragraph 6.4] for a review and [8] for an extended mathematical treatment of digital correlation). An adequate rejection requires a careful design of the correlator, and in particular of its front-end amplifiers [9–11]. The drawback of most effective amplifier design criteria is a poor stability of gain and frequency response. Hence, an automated in-line gain calibration subsystem has to be incorporated in the JNT.

We may call *relative* JNTs [7] those where the calibration signal is also given by Johnson noise of a resistor (the same or a different one), placed at a known reference temperature, which is typically T_{TPW}. A relative JNT measures the ratio $\mathcal{T}/\mathcal{T}_{TPW} = T/T_{TPW}$.

An *absolute* JNT measures $\mathcal{T}$ directly; therefore, the calibration signal has to be traceable to electromechanical SI units. Although in the past [3] a detailed proposal of an absolute JNT has been published, the only absolute JNT to have appeared in the literature is at the National Institute of Standards and Technology (NIST) [12–14]. In NIST's JNT the calibration signal is generated by a synthesized pseudorandom voltage noise source based on pulse-driven Josephson junction arrays; the calibration signal amplitude is thus directly linked to the Josephson fundamental constant K_J and the driving frequency of the Josephson array. In the absolute JNT described here, traceability to maintained SI electrical units is achieved by classical electrical metrology techniques.

3. Overview of the implementation

The block schematic of the JNT is shown in figure 1.

The probe resistor R, generating the Johnson noise e_N, is at temperature T, measured with a standard platinum resistance thermometer SPRT and a resistance meter M. The signal e_N is acquired by two identical acquisition channels in parallel, each one composed of an amplifier A and an analogue-to-digital converter ADC. Resulting digital codes are transmitted by an optical fibre interface to the processing computer PC, which implements a digital correlation spectrum analyzer algorithm.

The signal e_C is employed to periodically calibrate the analyzer gain, and injected in series with e_N. e_C is a pseudorandom noise, with the same bandwidth B of the measurement. It is generated by a PC and a digital-to-analogue converter DAC (also connected with the optical link). The waveform is measured by a voltmeter V, and reduced in amplitude by inductive voltage dividers IVD and an injection feedthrough transformer F. The measurements of V and M are acquired by PC through an IEEE-488 interface bus.

4. Details of the implementation

4.1. Probe resistor

The probe is a single resistor R, enclosed in a cylindrical screen and connected to the amplifiers A by a shielded four-wire cable (see figure 2). Presently a Vishay mod. VSR thick film resistor, having a nominal value of 1 kΩ, is employed. R is calibrated in dc regime, but a relative frequency deviation lower than 5×10^{-6} up to 10 kHz is expected [15].

4.2. Amplifiers

Amplifiers A are identical; each one is composed of two stages, giving an overall gain of ≈31 000. The first stage (see [16] for details) is a pseudo-differential, cascode FET amplifier in an open-loop configuration [11]. Its equivalent input voltage noise is ≈0.8 nV Hz$^{-1/2}$, and the bias current is 2 pA to 3 pA; the gain flatness is better than 1 dB over 1 MHz bandwidth. It is battery-powered (by separate battery packs for each channel to avoid residual correlations due to limited power-supply rejection ratio) and electrostatically shielded. Both first stages are placed in a mu-metal box which acts as a magnetic shield. A second conventional op-amp stage, working also as a rough bandpass filter and having a separate power supply, follows.

4.3. Spectrum analyzer

The ADCs (National Instruments mod. 4462: 24 bit resolution, 204.8 kHz maximum sampling frequency, synchronous sampling of the channels) are embedded in a PXI rack. The samples are acquired continuously and transmitted by an optical fibre link interface (National Instruments mod. 8336) to the PC, and grouped in *segments* having up to 2^{18} samples each. A digital cross-correlation algorithm based on fast-Fourier transform computes and averages spectra $C(f_k)$ having up to 2^{17} discrete frequency points f_k. Acquisition and computation are performed in parallel to optimize the measurement time.

4.4. Calibration

The calibration subsystem is shown in figure 2.

In the present setup we chose to inject the calibration signal e_C in series with the Johnson noise e_N during the calibration phase, at variance with the standard method of alternately measuring e_C and e_N. The advantage is a simplification

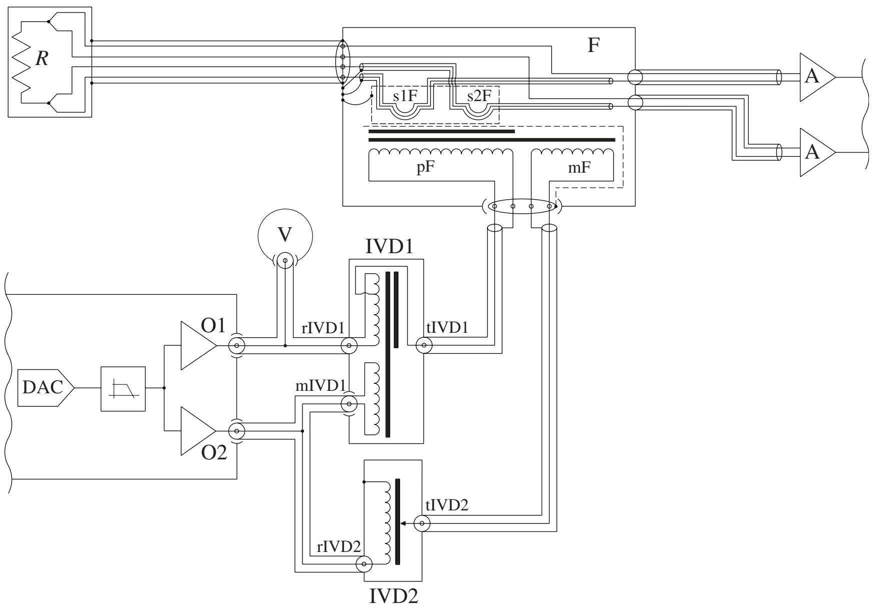

Figure 2. Detailed schematic of the calibration subsystem; see text for details.

in the layout, since no low-signal switching device is required; moreover, it is easier to keep electromagnetic interference under control. On the other hand, the effect of possible spectrum analyzer non-linearities has to be carefully considered [13].

A commercial DAC (National Instruments mod. 6733 board, 16 bit resolution, 1 MHz maximum sampling frequency, synchronized with the spectrum analyzer ADCs and embedded in the same PXI rack) generates the calibration waveform, which goes through an anti-alias filter (a 6-pole analogue Butterworth lowpass filter with 30 kHz bandwidth), and is buffered by two identical amplifiers with outputs O1 and O2 (each amplifier is provided with a dc output restoration circuit [17] to drive electromagnetic devices).

The signal is generated at an amplitude $V \approx 300\,\mathrm{mV}$, measured at output O1 with a calibrated thermal voltmeter V: presently, a Fluke mod. 8506A voltmeter is employed. Because of its limited accuracy and stability, the 8506A reading is compared, immediately before and after each experiment, with the reading of a Fluke mod. 5790A ac measurement standard, traceable to the national standard of ac voltage[2].

After generation, the calibration waveform is scaled in amplitude (presently, by a factor of 12 000). Such a large scaling factor is obtained by two electromagnetic devices: an inductive voltage divider (IVD1) having a nominal ratio of 100 : 1 and an injection transformer (F) with a nominal ratio of 120 : 1. Both IVD1 and F ratios are presently not calibrated, and the nominal turn ratio is employed in data processing.

The two-stage construction [19] of both IVD1 and F permits us to

- achieve a ratio close to nominal and with a high stability;
- increase the equivalent input impedance and reduce the equivalent output impedance. This permits minimization of loading errors caused by the cascading, and also the distortion of the output waveform.

IVD1 is a two-stage divider, with a magnetizing winding mIVD1 and a ratio winding rIVD1 with an output tap tIVD1 (details of the construction can be found in [20]). F is a two-stage feedthrough transformer, with a magnetizing winding mF and a primary winding pF, and two single-turn secondary windings s1F and s2F (wound with opposite polarities) which inject the calibration signal e_C in series with each connection of R to the amplifiers A.

The output O1, measured by the voltmeter V, is connected to rIVD1, whose tap tIVD1 is in turn connected to pF. The output O2 is employed to energize mIVD1 and mF; to obtain the correct magnetization voltage for mF, an auxiliary single-stage inductive voltage divider IVD2 (having a ratio winding rIVD2 with an output tap tIVD2 and the same nominal ratio of IVD1) is employed.

The calibration signal e_C is a pseudorandom noise, continuously recycled, having the power spectrum of a uniform frequency comb (see figure 3). The duration of each sample segment is a multiple of the repetition period of the calibration signal, and since ADC and DAC sampling rates are commensurate and derived from the same clock, no spectral leakage occurs in the spectrum analyzer output.

At variance with the NIST calibration waveform, whose comb covers the entire bandpass of the analyzer, e_C is band-limited: the comb frequencies uniformly cover the chosen measurement bandwidth B. The sine-wave amplitudes are carefully adjusted in order to have a flat comb (relative deviations from the average amplitude better than 1×10^{-3}) at the output of mIVD1. Since the sine waves have a relative phase chosen at random, e_C has an approximate Gaussian distribution of amplitudes.

A possible source of error is related to the different physical locations of sources of e_N (R within the thermostat) and e_C (the feedthrough transformer F), and correspondingly

[2] Unfortunately, the 5790A has a periodically fluctuating input impedance [18], which causes glitches in the acquisition, and cannot be directly employed during the measurement.

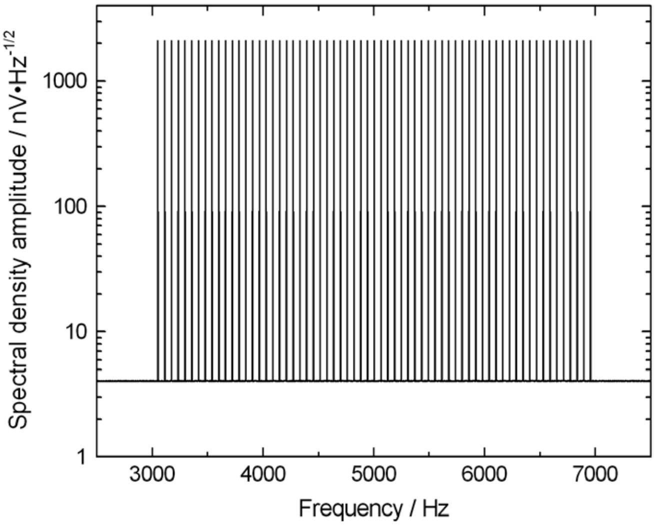

Figure 3. The calibration signal e_C for a bandwidth $B = 3$ kHz to 7 kHz. The baseline is the Johnson noise e_N.

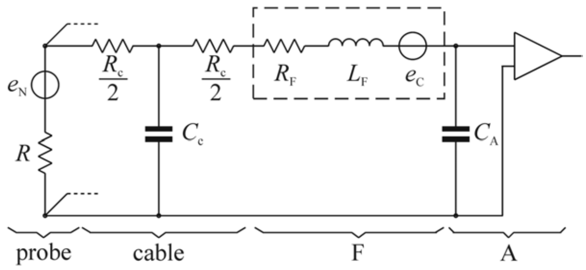

Figure 4. Simplified electrical schematic of the connection from R to amplifier input A, to evaluate the transfer functions of thermal noise signal e_N and calibration signal e_C (only one connection out of two is shown). R_c and C_c are the resistance and capacitance of the connecting cable (arranged in a T-network model); R_F and L_F are the parasitic resistance and inductance of the secondary winding of F; C_A models the equivalent input capacitance of A, of F and of the connection between the two. Measurements on the present setup give the following estimates: $R_c = 100\,\mathrm{m\Omega}$; $C_c = 30$ pF; $R_F = 10\,\mathrm{m\Omega}$; $L_F = 50$ nH; $C_A = 40$ pF.

on different electrical locations along the cable to A; therefore, the two transfer functions to the A input can differ. A simplified electrical model is shown in figure 4. For the present setup and the bandwidth B considered in the experiment, the error computed with the model of figure 4 is lower than 2×10^{-6}.

4.5. Thermometry

Resistor R is at the moment not thermostatted, but simply kept in an isothermal equalization block at room temperature. Temperature T_{90} is measured with a 100 Ω standard platinum resistance thermometer (SPRT), a Minco mod. S1060-2, calibrated at the fixed points of the ITS-90, as maintained at INRIM [21]. The meter M measuring the SPRT is presently an Agilent Tech. mod 3458A, option 002, whose calibration is traceable to the Italian standard of dc resistance.

5. Measurement procedure

The measurement consists of n repeated cycles, labeled $j = 1, \ldots, n$, each one composed of two phases:

- measurement of the power spectral density $N^j(f_k)$ (obtained by averaging spectra of m_N segments) when only e_N is present at the spectrum analyzer input. Reference SPRT temperature T_{90}^j is also measured during this phase;
- measurement of the power spectral density $C^j(f_k)$ (average of m_C segments) when both e_N and e_C are present. The calibration voltage V^j is also measured during this phase.

The measurement model is

$$G^j = \frac{1}{D\,V^j}\left\{\Delta f \sum_{f_k \in B}\left[C^j(f_k) - N^j(f_k)\right]\right\}^{1/2}, \qquad (1)$$

$$\mathcal{T}^j = \frac{1}{4R\left(G^j\right)^2}\Delta f \sum_{f_k \in B} N^j(f_k), \qquad (2)$$

$$\Delta T^j = k_B^{-1}\mathcal{T}^j - T_{90}^j, \qquad \delta^j = \frac{\Delta T^j}{T_{90}^j}. \qquad (3)$$

Here f_k are the (equally spaced) discrete frequency points within the chosen measurement bandwidth B and $\Delta f = f_{k+1} - f_k$ is the corresponding frequency bin width. D is the total scaling ratio of the electromagnetic divider chain. Equation (1) estimates the equivalent voltage gain G^j, averaged over B of the analyzer during cycle j (may be different for different j because of electronic drifts). Gain G^j is employed in equation (2), derived from the Johnson noise expression, to estimate the JNT temperature reading $\mathcal{T}^j$ in energy units.

Equation (3) gives the deviation ΔT^j in kelvin, and the corresponding relative deviation δ^j, between $\mathcal{T}^j$ and the SPRT reference temperature T_{90}^j (assuming a known Boltzmann constant k_B).

6. Results

As an example of results, the following refers to a continuous acquisition run (the parameters of the acquisition are $n = 1200$ cycles, each of 2^{17} points at 200 kHz sampling frequency, $m_N = 200$, $m_C = 50$, $B = 3$ kHz to 7 kHz; the calibration signal has a length of 2^{16} codes with 500 kHz sampling rate). Total measurement time is 2.3×10^5 s (about 2.7 days).

A typical spectrum of $N(f_k)$ (averaged over j) and the corresponding autospectra of the two channels (rescaled with the same G_j) are shown in figure 5.

For this experimental run, the relative deviations δ^j have a mean $\delta = -33\,\mu\mathrm{K\,K^{-1}}$ with a standard deviation $\sigma_\delta = 40\,\mu\mathrm{K\,K^{-1}}$. Such an experimental value for σ_δ is near (+24%) the theoretical prediction for the Type A uncertainty of a measurement performed with an ideal absolute thermometer[3] measuring over the same bandwidth B for the same total time τ.

[3] That is, having noiseless amplifiers and an *a priori* known and stable gain.

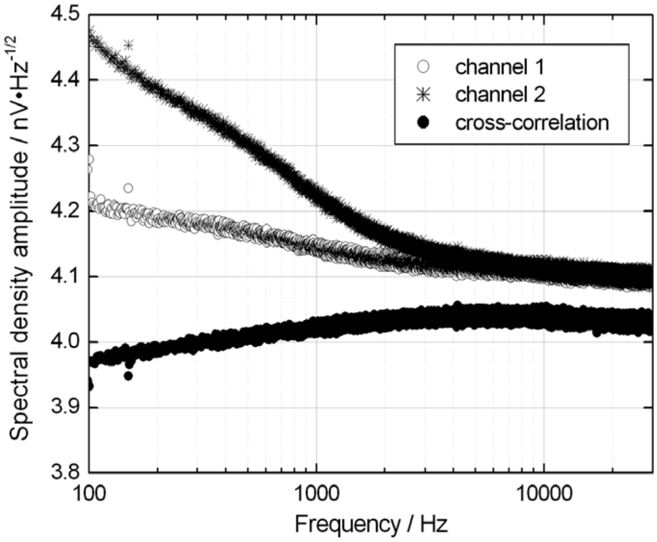

Figure 5. Amplitude spectra of the cross-correlation signal $N(f_k)$ and of the autocorrelation of the two spectrum analyzer acquisition channels separately. The flicker noise of A is apparent in the autospectra. The shape of $N(f_k)$ is slightly convex because of the bandpass filtering in the second stage of A.

More interestingly, σ_δ is somewhat *lower* (−14%) than the theoretical prediction for an ideal *relative* noise thermometer, if τ includes the time required for calibration with a known reference temperature[4].

Figure 6 shows these same conclusions in a graphical form, but when Allan standard deviations are compared; the noise of δ is still approximately white, therefore the JNT Type A uncertainty is at the moment limited only by the acquisition time. The time for a continuous measurement run is in turn limited by the battery charge (the run here presented is close to this limit) but the results of several runs can be averaged together.

An interesting performance test [22] is the measurement, instead of the noise e_N of the resistor R, of two independent noises e_{N1} and e_{N2} generated by two resistors R_1 and R_2, with $R_1 = R_2 = R$ and mounted in a probe having electrical properties similar to that of R. An ideal spectrum analyzer outcome would be a null spectrum at any frequency; the spectrum measured gives the magnitude of the systematic errors due to undesired residual correlation effects, introduced by the injection transformer F (possible residual couplings between secondary windings s1F and s2F, thermal noise in the magnetic core, etc), couplings between the amplifiers or ADC channels, broadband interferences. The test, however, does not rule out the existence of all residual correlations [3, 9, 11] that could occur when a single resistor is measured.

[4] The subject is extensively treated in [8]: in short, when a JNT is calibrated with a reference temperature, a truly random noise is measured; in our JNT (as in the NIST one), the calibration is performed with a *pseudorandom* noise e_C which has no intrinsic statistical fluctuations. The calculations given in [8] assume that e_C and e_N are alternatively switched at the spectrum analyzer input. Since in our setup e_C is added to e_N, results of [8] must be slightly adjusted. For example, equation (30) becomes

$$\ldots = \frac{1}{2\tau\Delta f_C}\left[\left(1+\frac{\sigma_{n1}^2}{\sigma_{sum}^2}\right)\left(1+\frac{\sigma_{n2}^2}{\sigma_{sum}^2}\right)+1-2\frac{\sigma_C^4}{\sigma_{sum}^4}\right], \quad (4)$$

where $\sigma_{sum}^2 = \sigma_C^2 + \sigma_N^2$ is the variance of the signal $e_{sum} = e_C + e_N$ (other symbols follow the notation of [8]). With the amplitude of e_C chosen for the experiment described, the difference between the original and the modified equation outcomes is negligible.

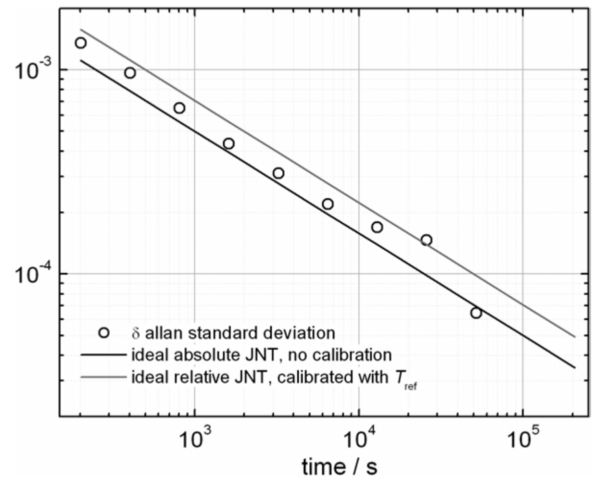

Figure 6. Allan standard deviation of the JNT error $\delta_j = \Delta T^j/T_{90}$ compared with the corresponding theoretical predictions for an ideal absolute thermometer and an ideal relative thermometer calibrated against a reference temperature T_{ref}.

In this setup, the residual correlation appears to have a quadratic frequency dependence which when integrated on B gives a systematic deviation lower than $10\,\mu K\,K^{-1}$.

Consistency tests for different run parameters (bandwidth B extension, sampling rate, R value, e_C/e_N ratio, choice of m_N and m_C, etc) require great experimental effort, and will be conducted in a systematic way on a future version of the thermometer (see section 8) for which we expect improved performances.

7. Uncertainty

The JNT uncertainty estimation includes a large number of terms. While some of them are related to the well-established instrument properties and calibration techniques (thermometry, resistance and ac voltage measurement), others are a matter of careful theoretical evaluations and ad-hoc experiments on the acquisition chain of the thermometer [9, 10] and in particular of the properties of the input amplifiers [11]. Even the data processing algorithms may cause unexpected systematic errors, as has been very recently pointed out [8]. We did not yet go through those hard tasks. Therefore, the uncertainty budget given in table 1 for the relative reading error δ is intended only as a tool to identify further goals for improvement: some contributions are truly related to our JNT, others are simply taken from the literature.

If the estimation of table 1 is provisionally trusted, the relative difference between the JNT and the resistance thermometer readings δ has an uncertainty $u(\delta) = 58\,\mu K\,K^{-1}$, whose main contribution comes from the JNT reading. Such a result can be compared with the recent estimate $u(\delta) = 25\,\mu K\,K^{-1}$ of the NIST absolute JNT at TPW [14], or with those of a number of (relative) acoustic thermometry results [23, 24], which consistently estimate $\delta = 12\,\mu K\,K^{-1}$ with a

Table 1. Uncertainty budget for the thermometer relative error δ.

	Type	$\mu K\,K^{-1}$	mK (at 300 K)	Note
JNT uncertainty				
Probe				
Resistance calibration	B	4.9	1.5	Direct reading 3458A, 1 kΩ range, 90 d cal
Resistance drift	B	2.0	0.6	Between recalibrations
Ac–dc correction	B	5.0	1.5	[14]
Probe total	B	7.3	2.2	
Calibration signal				($\times 2$ sensitivity coefficient)
Voltmeter calibration	B	25.4	7.6	5790A, 2.2 V scale, 90 d, over B
Voltmeter stability	B	10.0	3.0	8506A drift
Main IVD ratio	B	5.8	1.7	Max error of 1×10^{-7} (referred to input) over B
Injection transformer ratio	B	20.8	6.2	Max error of 3×10^{-7} (referred to input) over B
Transmission line error	B	2.0	1.6	
Calibration, total	B	34.9	10.5	
Amplifiers and ADC				
EMI	B	10.0	3.0	[13]
Residual correlation	B	10.0	3.0	Experiments and [13]
Non-linearity	B	5.0	1.5	[13]
Sampling frequency	B	1.4	0.4	Clock specs
Amplifiers and ADC, total		15.1	4.5	
u_R, Type B, RSS	B	38.7	11.6	
u_R, Type A	A	40.4	12.1	2.3×10^5 s acquisition time
u_R, Type A + B		55.9	16.8	
Thermometry				
SPRT calibration	B	1.0	0.3	Fixed points calibration ($U = 0.5$ mK at 300 K)
Resistance meter	B	8.7	2.6	Direct reading 3458A, 100 Ω range, 90 d cal
Self-heating	B	6.0	1.8	Estimate (not measured)
Immersion	B	1.5	0.5	At room temperature
Stability	B	5.0	1.5	Over one cycle
Thermometry, total	B	11.8	3.5	
Comparison				
RSS		58.4	17.5	JNT and thermometry uncertainty

relative uncertainty as low as $2\,\mu K\,K^{-1}$ near the gallium fixed point (≈303 K).

8. Conclusion and perspectives

Looking at table 1, we see that a number of uncertainty contributions come from specifications of the commercial instruments employed or, more generally, from measurements for which primary metrology know-how provides better solutions. Therefore, there is room for improvements. We are working on the following:

- the development of a thermostat to perform measurements by varying T over a range that includes T_{TPW} [25];
- improvements in thermometry measurement setup with the implementation of a resistance bridge;
- the calibration of dividers over B under loading condition;
- improvements in the measurement of V^j with an automated ac–dc transfer measurement system based on a multijunction thermal converter [26];
- the increase in the measurement bandwidth to $B \approx 20$ kHz;
- an improved modelling of the analogue part of the analyzer, to correct for transmission line errors;
- larger battery packs for an extended measurement time.

With these improvements, the measurement uncertainty should drop to the level of $10\,\mu K\,K^{-1}$; a measurement at T_{TPW} will permit the determination of k_B with the same uncertainty.

Acknowledgments

The authors are indebted, for their help in the development of the experiment and fruitful discussions, to their INRIM colleagues R Gavioso, E Massa, F Manta and A Merlone; and to M Ortolano (Politecnico di Torino, Italy).

References

[1] Johnson J B 1928 Thermal agitation of electricity in conductors *Phys. Rev.* **32** 97–109

[2] 2005 Recommendation T2: new determinations of thermodynamic temperature and the Boltzmann constant *Working Documents of the 23rd Meeting of the Consultative Committee for Thermometry (Sèvres, 2005)* BIPM document CCT/05-31

[3] Storm L 1986 Precision measurements of the Boltzmann constant *Metrologia* **22** 229–34

[4] Fellmuth B, Gaiser Ch and Fischer J 2006 Determination of the Boltzmann constant—status and prospects *Meas. Sci. Technol.* **17** R145–9

[5] Mohr P J, Taylor B N and Newell D B 2008 CODATA recommended values of the fundamental physical constants: 2006 *Rev. Mod. Phys.* **80** 633–730

[6] Mohr P J, Taylor B N and Newell D B 2008 CODATA recommended values of the fundamental physical constants: 2006 *J. Phys. Chem. Ref. Data* **37** 1187–284

[7] White D R *et al* 1996 The status of Johnson noise thermometry *Metrologia* **33** 325–35

[8] White D R, Benz S P, Labenski J R, Nam S W, Qu J F, Rogalla H and Tew W L 2008 Measurement time and statistics for a noise thermometer with a synthetic-noise reference *Metrologia* **45** 395–405

[9] White D R 1984 Systematic errors in a high-accuracy Johnson noise thermometer. *Metrologia* **20** 1–9

[10] Storm L 1989 Errors associated with the measurement of power spectra by the correlation technique *Noise in Physical Systems, Including 1/f Noise, Biological Systems and Membranes: 10th Int. Conf. Proc. (Budapest, Hungary, 21–25 August 1989)* pp 551–60

[11] White D R and Zimmermann E 2000 Preamplifier limitations on the accuracy of Johnson noise thermometers *Metrologia* **37** 11–23

[12] Sae Woo Nam, Benz S P, Dresselhaus P D, Tew W L, White D R and Martinis J M 2003 Johnson noise thermometry measurements using a quantized voltage noise source for calibration *IEEE Trans. Instrum. Meas.* **52** 550–4

[13] White D R and Benz S P 2008 Constraints on a synthetic noise source for Johnson noise thermometry *Metrologia* **45** 93–101

[14] Benz S P, Qu J, Rogalla H, White D R, Dresselhaus P D, Tew W L and Nam S W 2009 Improvements in the NIST Johnson noise thermometry system *IEEE Trans. Instrum. Meas.* **58** 884–90

[15] Bohacek J 2006 Reference resistors for calibration of wideband LCR meters *Proc. 18th IMEKO World Congress on Metrology for a Sustainable Development* (*Rio de Janeiro, Brazil, 17–22 September 2006*) p 00594

[16] Callegaro L, Pisani M and Pollarolo A 2008 Very simple FET amplifier with a voltage noise floor less than 1 nV/$\sqrt{\text{Hz}}$ arXiv:0811.2866 [physics.inst-det]

[17] Stitt R M 1991 AC coupling instrumentation and difference amplifiers *AB-008A Burr-Brown Application Bulletin*

[18] Simonson P and Rydler K-E 1996 Loading errors in low voltage ac measurements *Precision Electromagnetic Measurements Conf. Digest CPEM'96* (*Braunschweig, Germany, 17–20 June 1996*) pp 572–3

[19] Deacon T A and Hill J J 1968 Two-stage inductive voltage dividers *Proc. IEE* **115** 888–92

[20] Callegaro L, Bosco G C, D'Elia V and Serazio D 2003 Direct-reading absolute calibration of ac voltage ratio standards *IEEE Trans. Instrum. Meas.* **52** 380–3

[21] Marcarino P, Steur P P M and Dematteis R 2003 Realization at IMGC of the ITS-90 fixed points from the argon triple point upwards *Temperature: its Measurement and Control in Science and Industry* vol VII *8th Temperature Symp. (Chicago, IL) AIP Conf. Proc.* **684** 65–70

[22] Zhang J T and Xue S Q 2008 Investigation of the imperfection effect of correlation on Johnson noise thermometry *Metrologia* **45** 436–41

[23] Benedetto G, Gavioso R M, Spagnolo R, Marcarino P and Merlone A 2004 Acoustic measurements of the thermodynamic temperature between the triple point of mercury and 380 K *Metrologia* **41** 74–98

[24] Ripple D C, Strouse G F and Moldover M R 2007 Acoustic thermometry results from 271 to 552 K *Int. J. Thermophys.* **28** 1789–99

[25] Merlone A, Iacomini L, Tiziani A and Marcarino P 2007 A liquid bath for accurate temperature measurements *Measurement* **40** 422–7

[26] Pogliano U, Trinchera B and Francone F 2009 Reconfigurable unit for precise RMS measurements *IEEE Trans. Instrum. Meas.* **58** 827–31